Published in final edited form as:
Biomaterials. 2013 October ; 34(31): 7683–7693. doi:10.1016/j.biomaterials.2013.06.057.

Peptide Targeted Tripod Macrocyclic Gd(III) Chelates for Cancer Molecular MRI

Zhuxian Zhou[a], **Xueming Wu**[a], **Adam Kresak**[b], **Mark Griswold**[c], and **Zheng-Rong Lu**[a,*]

[a]Department of Biomedical Engineering, Case Western Reserve University, Cleveland, OH 44106

[b]Case Comprehensive Cancer Center, Case Western Reserve Univeristy, Cleveland, OH 44106

[c]Department of Radiology, Case Western Reserve University, Cleveland, OH 44106

Abstract

Rational design and develop of targeted contrast agents binding to cancer-related proteins will achieve more accurate cancer diagnosis and prognosis by magnetic resonance (MR) imaging. CREKA is a tumor-homing pentapeptide (Cys-Arg-Glu-Lys-Ala) specifically homes to fibrin-fibronectin complexes abundantly expressed in tumor microenvironment. In this study, we developed and evaluated a CREKA peptide targeted multiplexed Gd-MR probe (CREKA-Tris-Gd(DOTA)) for MR imaging of breast tumors. CREKA and azide bearing Gd(III) was attached to a maleimide-functional trialkyne scaffold via thiol-maleimide and azide-alkyne click chemistry, respectively. CREKA-Tris-Gd(DOTA) has a well-defined structure with a molecular weight of 2914 Da. The T_1 relaxivity of CREKA-Tris-Gd(DOTA) is 8.06 $mM^{-1}s^{-1}$ per Gd (24.18 $mM^{-1}s^{-1}$ per molecule) at room temperature and 3 T. Fluorescence imaging showed high binding specificity of CREKA to a 4T1 breast tumor model in mice while it was not found for the scrambled CREKA (CERAK). The CREKA peptide-targeted contrast agent resulted in greater contrast enhancement than the corresponding CERAK agent and the commercialized contrast agent Prohance™ in tumor at a dose of 0.1 mmol Gd/kg in female athymic mice bearing 4T1 breast carcinoma xenograft. This small molecular contrast agent was easily excreted from body after imaging indicated low toxicity. The targeted MRI contrast agent has a potential for specific cancer molecular imaging with MRI.

1. Introduction

Effective imaging of cancer-related molecular biomarkers is essential for early and accurate diagnosis and prognosis of the disease. Magnetic resonance imaging (MRI) is a clinical imaging modality effective for anatomical and functional imaging of soft tissues, including solid tumors.[1] Stable Gd(III) chelates with low toxicity are most commonly used as MRI contrast agents to alter the water proton relaxation rate in the tissues of interest and to

Corresponding author: Z. R. Lu, zxl125@case.edu, fax: 216-368-4969.

enhance image contrast in the surrounding tissues.[2, 3] Conjugation of tumor-specific targeting agents to the stable Gd(III) based contrast agents can improve the binding of the agents to cancer biomarkers and produce signal enhancement around the biomarkers for cancer molecular imaging.[4, 5] However, contrast enhanced MRI has not been effective for molecular imaging of biomarkers expressed on cancer cell surfaces because of its low sensitivity, the low concentration of the biomarkers and insufficient signal enhancement. In order to produce MRI detectable signal enhancement, a relatively large amount of Gd(III) chelates are often loaded on targeted nanoparticles to increase the concentration of the agents around cancer cellular biomarkers.[6-10] Although targeted nanoparticles loaded with Gd(III) chelates can produce significant specific tumor enhancement,[6, 11-13] clinical development of these agents is hindered by their slow and incomplete elimination from the body, which could result in toxic side effects, including systemic nephrogenic fibrosis.[14, 15]

Innovative design of safe and effective targeted contrast agents and identification of suitable molecular targets are critical for MR cancer molecular imaging. Small molecular targeted Gd(III) chelates eliminate rapidly from the body and have better safety profiles over nanosized agents.[16, 17] Tumor tissue has a unique microenvironment in which various cancer related proteins, e.g. tenascin[18] and oncofetal fibronectin[19], are highly expressed in the tumor extracellular matrix to facilitate cancer cell survival, proliferation and metastasis. These extracellular proteins could be viable biomarkers for MR cancer molecular imaging. Small molecular targeted Gd(III) chelates specific to these biomarkers can be developed for safe and effective molecular MRI.[20-22] A sufficient amount of small molecular targeted agents can bind to the abundant tumor biomarkers generating robust signal increase for detection and quantification of the biomarkers with MRI. Unbound agents can be readily excreted from the circulation, resulting in reduced background noise for accurate molecular imaging and minimal tissue retention.[23]

In this work, we designed and synthesized a pentapeptide CREKA (Cys-Arg-Glu-Lys-Ala) macrocyclic Gd(III) chelate conjugate with a tripod spacer, CREKA-Tris(Gd-DOTA)$_3$, as a small molecular targeted contrast agent for molecular MRI of a biomarker in the tumor microenvironment (Scheme 1). A macrocyclic Gd(III) chelate (Gd-DOTA monoamide) was chosen for the peptide conjugated contrast agents because of its superior kinetic stability compared to the linear Gd(III) chelates such as Gd-DTPA.[24-26] CREKA specifically bound to fibrin-fibronectin complexes in tumor extracellular matrix with little binding in normal tissues.[27, 28] We verified the binding of the peptide to the fibrin and fibronectin in 4T1 breast cancer tissue and determined the effectiveness of the agent for MR cancer molecular imaging in a mouse 4T1 breast cancer model.

2. Materials and methods

2.1. Materials

All reagents were used without further purification unless otherwise stated. Benzotriazol-1-yl-oxytripyrrolidinophosphonium hexafluorophosphate (PyBOP), 1-hydroxybenzotriazole hydrate (HOBt), 2-chlorotritylchloride resin and all of the Fmoc protected amino acids were purchased from Chem-Impex International, Inc. Fmoc-12-amino-4,7,10-trioxadodecanoic

acid (Fmoc-NH-$(PEG)_2$-COOH) were purchased from EMD Chemicals Inc. (Gibbstown, New Jersey). Anhydrous *N*,*N*-diisopropylethyl amine (DIPEA) and *N*,*N*-dimethylformamide (DMF) were purchased from Alfa Aesar (Ward Hill, MA). Trifluoroacetic acid (TFA) was purchased from Oakwood Products, Inc. Sulfo-Cy5.0 NHS ester was purchased from Lumiprobe (Hallandale Beach, FL). Gd(III) Azido-DOTA monoamide complex (Azido-(Gd-DOTA)) was synthesized according to the literature.[29]

2.2. General methods of characterization

^1H and ^{13}C NMR spectra were obtained on a 300 MHz Varian Gemini NMR spectrometer or a 600 MHz Varian Inova NMR spectrometer with deuterated solvent as noted. Matrix-assisted laser desorption/ionization time-of-flight (MALDI-TOF) mass spectra were acquired on a Bruker Autoflex III MALDI-TOF MS in a linear mode with 2,5-dihydroxybenzoic acid (2,5-DHB) as a matrix. Ion-pairing reverse-phase HPLC (RP-HPLC) was performed on an Agilent 1100 series HPLC system fitted with a Beckman Coulter Ultrasphere ODS 4.6 mm × 25 cm, 5 μm pore size column. Gradient elution was used to characterization and purification. Eluent A was water, B was acetonitrile and flow rate was 1.0 mL/min. The detection of eluted samples was performed at 210 nm. Cy5.0 conjugated peptides were purified by HPLC method 1: 0-10 min 100% A, 10-40 min 60% A, 40-50 min 100% A. Products were collected at 27 min. The purity of the contrast agents were studied by HPLC method 2: 0-10 min 100% A, 10-30 min 60% A, 30-35 min 0% A, 35-40 min 0% A, 40-45 min 100% A. Relaxation times of the aqueous solution of the contrast agents with different concentrations were measured at 60 MHz (1.5 T) using a Bruker minispec relaxometer at 37 °C. T_1 was measured with an inversion–recovery pulse sequence. T_2 was measured using a Carr-Purcell-Meiboom-Gill sequence with 500 echoes collected. The T_1 and T_2 relaxivities of the agents were calculated from the slopes of the plots of $1/T_1$ and $1/T_2$ versus the Gd concentrations.

2.3. Synthesis of Maleimido-Tris-Propargyl (Scheme 2)

2.3.1. Synthesis of tris[(propargyloxy)methyl]aminomethane (Tris-Propargyl, 3)—

Boc-Tris-Propargyl[30] (**2**, 5 g, 14.9 mmol) was dissolved in a mixture solvent of dichloromethane (15 mL) and trifluoroacetic acid (15 mL). The mixture was stirred at room temperature for 2 h. The solvent was removed by rotary evaporator to get **3** as colorless oil (4.9 g, yield 100%). ^1H NMR (300 MHz, $CDCl_3$, δ): 2.49 (t, 3H, C≡CH), 3.73 (s, 6H, C_qCH_2O), 4.20 (d, 6H, $OCH_2C{\equiv}CH$), 8.12 (br, 2H, NH_2).

2.3.2. Synthesis of pentafluorophenyl 3-(2,5-dioxo-2,5-dihydro-1H-pyrrol-1-yl)propanoate (Maleimido-propionic-PFP, 5)—

Maleimido-propionic acid[31] (**4**, 11.5 g, 68 mmol) and pentafluorophenol (12.5 g, 68 mmol) was dissolved in dioxane (150 mL). DCC (15.4 g, 74.8 mmol) in dioxane (50 mL) was added to this solution and the mixture was stirred at room temperature overnight. The solution was filtered and the solvent was removed by rotary evaporator. The product was purified by recrystallization in acetone/hexane to get **5** as white sheet-like crystal (21 g, 92%). ^1H NMR (300 MHz, $CDCl_3$, δ): 3.05 (t, 2H, CH_2CO), 3.96 (t, 2H, NCH_2), 6.75 (s, 2H, CH=CH).

2.3.3. Synthesis of N-(1,3-bis(prop-2-yn-1-yloxy)-2-((prop-2-yn-1-yloxy)methyl)propan-2-yl)-3-(2,5-dioxo-2,5-dihydro-1H-pyrrol-1-yl)propanamide (Maleimido-Tris-Propargyl, 6)—Tris-Propargyl (**3**, 7.9 g, 23.9 mmol) and Maleimido-propionic-PFP (**5**, 8.0 g, 23.9 mmol) was dissolved in DMF (50 mL). DIPEA (8.3 mL, 47.8 mmol) was added to the solution and the mixture was stirred at room temperature under N_2 overnight. Dichloromethane (300 mL) was added to the solution and the mixture was washed with water (5 × 500 mL) and brine (1 × 300 mL). The organic solution was collected, dried over Na_2SO_4 and the solvent was removed by rotary evaporator. The product was purified by column chromatography (SiO_2, CH_2Cl_2/ethyl acetate 3:1) to get **6** as colorless viscous oil (7.5 g, yield 82%). ^{1}H NMR (300 MHz, $CDCl_3$, δ): 2.44 (t, 3H, C≡CH), 2.50 (t, 2H, CH_2CO), 3.81 (s, 8H, NCH_2 + C_qCH_2O), 4.12 (d, 6H, $OCH_2C{\equiv}CH$), 5.70 (br, 1H, NH), 6.69 (s, 2H, CH=CH). ^{13}C NMR (600 MHz, $CDCl_3$) δ 34.44 (1C, $\underline{C}H_2CO$), 35.45 (1C, $N\underline{C}H_2$), 58.84 (3C, $O\underline{C}H_2C{\equiv}CH$), 59.53 (1C, $NH\underline{C}_q$), 68.55 (3C, $C_q\underline{C}H_2O$), 74.99 (3C, C≡$\underline{C}$H), 79.76 (3C, $CH_2\underline{C}{\equiv}CH$), 134.38 (2C, $\underline{C}H{=}\underline{C}H$), 169.86 (1C, $CH_2\underline{C}ONH$), 170.68 (2C, $CH\underline{C}ON$). MALDI-TOF (m/z, M^+): 386.74 (found), 386.15 (calcd).

2.4. Synthesis of CREKA-Tris(Gd-DOTA)$_3$ and scrambled CERAK-Tris(Gd-DOTA)$_3$ (Scheme 3)

CREKA·3TFA (250 mg, 0.26 mmol) and Maleimido-Tris-Propargyl (120 mg, 0.31 mmol) were dissolved in DMF (5 mL). To this solution, DIPEA (220 mg, 1.3 mmol) was added and the mixture was stirred under N_2 for 1 h. The solution was then poured into cold ethyl ether (100 mL) to precipitate the product. The product was collected, washed with ethyl ether and dried in vacuum. The yield of CREKA-Tris-Propargyl was 94%. MALDI-TOF (m/z, M^+): 991.80 (observed); 991.44 (calcd).

CREKA-Tris-Propargyl (200 mg, 0.2 mmol) and Azido-(Gd-DOTA) (512 mg, 0.8mmol) was dissolved in a mixed solvent of t-BuOH and water (t-BuOH, 5 ml; water, 8 ml). To this solution, $CuSO_4{\cdot}5H_2O$ (10 mg, 0.04 mmol) was added and the mixture was degassed and stirred under N_2 at room temperature for 24 h. The reaction was traced by MALDI-TOF until CREKA-Tris-Propargyl was completely conjugated the Gd-DOTA monoamide. The solution was dialyzed (MWCO = 1000) against 0.5% EDTA solution (1 L × 3) for 12 h and then against water (1L × 3) for 24 h. A colorless solid was obtained after freeze drying, with a yield of 61%. No free Gd(III) ions were detected with Xylenol orange in the final product. MALDI-TOF (m/z, $[M + H]^+$): 2913.58 (obsd); 2912.91 (calcd). ICP-OES (Gd^{3+} content): 15.68 % (obsd); 16.25% (calcd). A scrambled peptide control agent CERAK-Tris-(Gd-DOTA)$_3$ was synthesized by the same method with a yield of 63%. MALDI-TOF (m/z, $[M + H]^+$): 2913.79 (obsd); 2912.91 (calcd). ICP-OES (Gd^{3+} content): 16.01% (obsd); 16.25% (calcd).

2.5. Synthesis of Cy5.0-PEG-CREKA and Cy5.0-PEG-CERAK

Peptide CREKA with an N-terminal cysteine was synthesized using standard solid-phase peptide synthesis from Fmoc-protected amino acids on a 2-chlorotrityl chloride resin. At the end of the peptide synthesis, 10 mg (including resin, ~2.5 μmol) of NH_2-terminated CREKA resin was mixed with a DMF solution of Fmoc-NH-$(PEG)_2$-COOH (4.3 mg, 10 μmol),

PyBop (5.2 mg, 10 μmol), HoBt (1.4 mg, 10 μmol) and DIPEA (4 μL). The mixture was stirred at room temperature for 1 h and the resin was thoroughly washed with DMF. The protective group, Fmoc, was removed by reacting with 20% piperidine in DMF and the resin was thoroughly washed with DMF. Sulfo-Cy5.0 NHS ester (2 mg, 2.6 μmol) in DMF (0.1 ml) was then added to the resin and DIPEA (4 μL) was dropped to the solution. The mixture was stirred at RT under N_2 overnight. The resin was completely washed with DMF. The Cy5.0-PEG-CREKA was then removed from the resin using TFA solution (TFA 94%, 1,2-ethanedithiol 2.5%, triisobutylsilane 2.5%, water 1.0%). The crude product was precipitated out from ethyl ether and washed with ethyl ether. The product was purified by HPLC to get 1.2 mg.

2.6. Animal models

Six-week-old female BALB/c mice (Charles River) were cared at the Animal Core Facility of Case Western Reserve University according to an animal protocol approved by the CWRU Institutional Animal Care and Use Committee. 4T1-GFP-Luc2 breast cancer cell line was purchased from Caliper Life Sciences and maintained as recommended by the provider. The mice were anesthetized and 4T1-GFP-Luc2 breast cancer cells (1×10^6 in 40 μL PBS) were injected into the mammary fat pad to induce tumors. To monitor the growth of the 4T1-GFP-Luc2 breast tumors, the mice were intraperitoneally injected with D-luciferin (200 μL in PBS, 15 mg/mL). Ten minutes following the injection, mice were anesthetized by 2% isoflurane and imaged on Xenogen IVIS Lumina system (Caliper Life Sciences, Hopkinton, MA). The study was performed when the tumor size reached 0.5-1.0 cm in diameter in ~2 weeks.

2.7. Immunofluorescence

Tumors from mice injected with Cy5.0 labeled peptides were embedded in optimal cutting temperature compound (OCT) and cryosectioned into 5 μm slices. For fibronectin or fibrinogen immunostaining, tissues were stained with a rabbit anti-mouse fibronectin polyclonal antibody (Abcam) or a rabbit anti-mouse fibrinogen polyclonal antibody, followed by Rhodamine-Red conjugated goat anti-rabbit IgG (H+L) (Jackson Immuno Research Lab. West Grove, PA). Cell nucleus of the tissues were stained with 4’,6-diamidino-2-phenylindole (DAPI). Tissue slides were imaged on an Olympus FV1000 confocal laser scanning microscope. GFP was observed using 405 nm laser and the emission wavelength was read from 480 to 495 nm and expressed as green. DAPI was observed using 405 nm laser and the emission wavelength was read from 450 to 470 nm and expressed as blue. Rodamine-Red was observed using 543 nm laser and the emission wavelength was read from 560 to 620 nm and expressed as purple. Cy5.0 was observed using 635 nm laser and the emission wavelength was read from 655 to 755 nm and expressed as red.

2.8. In *vivo* MR tumor imaging

The MRI study was performed using a Bruker Biospec 7T MRI scanner (Bruker Corp., Billerica, MA, USA) with a volume radio frequency (RF) coil. Mice were anesthetized with a 2% isoflurane-oxygen mixture in an isoflurane induction chamber. A tail vein of mouse was catheterized with a 30 gauge needle connected with 1.6 m tubing filled with heparinized saline. The animal was then moved into the magnet and kept under inhalation anesthesia

with 1.5% isoflurane-oxygen via a nose cone. A respiratory sensor connected to a monitoring system (SA Instruments, Stony Brook, NY) was placed on the abdomen to monitor rate and depth of respiration. The body temperature was maintained at 37°C by blowing hot air into the magnet through a feedback control system. A group of 3 mice was used for each agent. Sagittal section images were acquired with a localizing sequence to identify the tumor location, followed by a 2D T_1-weighted gradient fat suppression sequence before injection. After pre-injection baseline MR imaging acquisition, the targeted agent, the non-targeted scrambled control or Prohance™ was injected at a dose of 0.1 mmol of Gd/kg by flushing with 80 μL of saline. T_1-weighted 2D axial images were then acquired at different time points after the injection for up to 30 min. Parameters of the 2D T_1-weighted gradient echo sequence were TR/TE = 151.2/1.9 ms, FOV = 3.0 cm, slice thickness = 1.2 mm, slice number = 12, average = 1, flip angle = 80°, matrix = 128 ×128.

2.9. Biodistribution study

Mice with 4T1-GFP-Luc2 breast tumors were sacrificed at 2 or 7 days postinjection. The organ and tissue samples, including the heart, liver, spleen, lung, kidneys, brain, skin, muscle, femur, and tumor were collected and weighed. The tissue samples were then cut into small pieces and mixed with ultrapure nitric acid (1.0 mL, 70%, EMD, Gibbstown, NJ). The tissue samples were liquefied for 1 week, and the solution was transferred to a centrifuge tube and centrifuged at 14 000 rpm for 5 min. The supernatant (0.2 mL) was diluted 10 times with deionized water and further centrifuged at 14 000 rpm for 5 min. The Gd(III) concentration in the supernatant solution was measured by ICP-OES. The average Gd(III) content in each organ or tissue was calculated from the measured Gd(III). The Gd content was calculated as the percentage of injected dose per gram of organ/tissues (% ID/g).

3. Results and Discussion

3.1. Synthesis and characterization of Small Peptide Targeted Macrocyclic Gd(III) Chelates

The targeted contrast agent CREKA-Tris(Gd-DOTA)$_3$ was synthesized according to the procedure described in Scheme 2 and 3. A tripod spacer, Maleimido-Tris-Propargyl, was first synthesized from TRIS to conjugate the peptide and three Gd(III) chelates (Scheme 2, Fig. 1). The amine group of TRIS was modified with a maleimide group for conjugating the peptide and the three hydroxyl groups were converted to trialkyne groups for attaching Azido-(Gd-DOTA). Multiple Gd(III) chelates were conjugated to each targeting moiety to improve targeting efficiency and contrast enhancement.[10, 29] Maleimido-Tris-Propargyl was characterized by ^{1}H NMR, ^{13}C NMR and Maldi-Tof MS spectrum (Fig. 1). CREKA-Tris(Gd-DOTA)$_3$ was readily synthesized by stepwise conjugation of CREKA and Azido-(Gd-DOTA) to the tripod spacer via thiol-maleimide and azide-alkyne click chemistry (Scheme 3). Importantly, the sulfhydryl group of the cysteine residue on CREKA is not essential for binding activity, thus conjugating CREKA to the spacer by cysteine would not result in the loss of binding activity.[28] CREKA-Tris(Gd-DOTA)$_3$ was characterized by MALDI-TOF mass spectrometry (Fig. 2) and its purity was verified by HPLC. The Gd(III) content was 16.01%, as determined by ICP-MS. A non-targeted control agent, CERAK-Tris(Gd-DOTA)$_3$ was similarly synthesized and characterized.

The plots of the T_1 and T_2 water proton relaxation rates at 1.5T versus the concentration of CREKA-Tris(Gd-DOTA)$_3$ or CERAK-Tris(Gd-DOTA)$_3$ are shown in Fig. 3. The T_1 relaxivity of CREKA-Tris-Gd(DOTA)$_3$ was 7.34 $mM^{-1}s^{-1}$ per Gd (22.02 $mM^{-1}s^{-1}$ per molecule) at room temperature and 1.5 T, 7.86 $mM^{-1}S^{-1}$ per Gd (23.58 $mM^{-1}s^{-1}$ per molecule) for CERAK-Tris(Gd-DOTA)$_3$. The relaxivity of both agents was much higher than that of clinical macrocyclic agents, Gd-DOTA (3.6 $mM^{-1}s^{-1}$) and Gd(HP-DO3A) (2.9 $mM^{-1}s^{-1}$) under the same condition, possibly because of the slow rotational motion of the complexes when Gd-DOTA monoamide was conjugated to the spacer.[32, 33] For agents with similar distribution, agents with higher relaxivity would provide equivalent contrast at a lower dose compared to lower relaxivity agents.[1]

3.2. CREKA Peptide Specific Binding to Fibrin-Fibronectin Complexes in Tumor Microenvironment

Specific binding ability of CREKA to fibrin and fibronectin in tumor tissue was further verified in Balb/c mice bearing orthotopic 4T1-GFP-Luc2 breast tumors. A fluorescent dye Cy5.0 was conjugated to the peptide via a short PEG spacer to obtain Cy5.0-PEG-CREKA (Fig. 4A). Cy5.0-PEG-CERAK was similarly prepared as a non-specific control. Mice bearing orthotopic 4T1-GFP-Luc2 were developed by inoculating cancer cells in the mammary fat pad and were used for the study 2 weeks after innoculation (Fig. 4B). Fig. 4C shows the bright-field and the fluorescent images of the major organs and tissues from the mice injected with the targeted and control probes 4 h after the injection. Strong red fluorescence was shown in the breast tumor from the mice injected with Cy5.0-PEG-CREKA, whereas little fluorescence was detected in the tumor from the mice injected with the control probe. The Cy5.0 fluorescence intensity in tumors from the mice injected with Cy5.0-PEG-CREKA was 3.86 times that of the tumor injected with the non-targeted peptide probe ($P < 0.01$) (Fig. 4D). No significant fluorescence was detected in healthy organs and tissues except the kidneys for both the targeted and control probes. The histological analysis of the organs from the mice injected with Cy5.0-PEG-CREKA further confirmed that CREKA specifically bound to tumor but not healthy tissues (Fig. 5). Significant Cy5.0 fluorescence was observed in the meshwork of the tumor tissues. Stronger fluorescence was found in the periphery of the 4T1 primary tumor than the interior (Fig. 6). The immunostaining of fibrin and fibronectin also indicated a similar distribution pattern of fibrin-fibronectin complexes in the tumor rim and interior.

Immunostaining of tumor sections with an antibody against fibronectin showed abundant fibronectin in the tumor extracelluar matrix of tumor meshwork. Fluorescence from Cy5.0-PEG-CREKA colocalized with fibronectin immunostaining (Fig. 7), which is consistent with the report.[28] The immunostaining of tumor sections with an antibody against fibrinogen indicated that the CREKA peptide probe also colocalized with fibrin in tumor tissue (Fig. 8). In comparison, the non-specific peptide probe resulted in very low Cy5 fluorescence in the tumor sections immunostained for fibronectin and fibrinogen (Fig. 7 and 8). These results confirmed that CREKA peptide can specifically target to the fibrin-fibronectin complexes in tumor extracellular matrix.

3.3. MR Tumor Molecular Imaging

In vivo MRI experiments were carried out with mice bearing orthotopic 4T1-GFP-Luc2 breast tumors 2 weeks after innoculation. Fat-suppressed T_1-weighted 2D spin echo MR images of the tumor enhanced with Prohance® (a commercial small molecular MRI agent with non-specific vascular and extravascular distribution), CERAK-Tris(Gd-DOTA)$_3$ and CREKA-Tris(Gd-DOTA)$_3$ are shown in Fig. 9A. The targeted contrast agent, CREKA-Tris(Gd-DOTA)$_3$, resulted in stronger contrast enhancement than both Prohance™ and CERAK-Tris(Gd-DOTA)$_3$, especially in the tumor periphery. The contrast-to-noise ratios (CNR) in the tumor rim or interior before and after the injection of contrast agents were measured and plotted in Fig. 9B for quantitative analysis of MR signal intensity. The targeted agent resulted in approximately two times more CNR than Prohance® and CERAK-Tris(Gd-DOTA)$_3$ in the tumor rim at the same dose. The targeted agent resulted in more prolonged contrast enhancement possibly due to specific target binding. In the first 15 minutes, CREKA-Tris(Gd-DOTA)$_3$ provided stable high contrast in the tumor periphery and then the contrast slowly decreased over time. At 30 minutes, CREKA-Tris(Gd-DOTA)$_3$ still produced strong enhancement and high CNR in the tumor periphery. By comparison, Prohance® and CERAK-Tris(Gd-DOTA)$_3$ only generated slight tumor contrast enhancement.

The small molecular targeted agent effectively bound to the biomarker in the tumor, resulting in strong tumor contrast enhancement, especially in the tumor periphery which is rich with angiogenic vasculature. The observation validated the hypothesis that abundant presence of the biomarker in tumor extracelullar matrix allowed the binding of a sufficient amount of the small targeted Gd(III) chelates to generate detectable signal enhancement for effective MR molecular imaging. Rapid clearance of unbound targeted agent from blood circulation reduced background signal, as evidenced by the maximum tumor CNR at 10 minutes post-injection and reduced signal intensity in the normal tissues. The effectiveness of the targeted agent for MR molecular imaging was demonstrated on a high-field animal scanner (7T), which is normally less effective for contrast enhanced T1 weighted imaging than relatively low field clinical MRI scanners (1.5 and 3T). The peptide targeted contrast agent has a potential to produce more significant contrast enhancement for T_1 weighted molecular imaging on clinical scanners.

3.4. Biodistribution and renal clearance

To investigate the retention of the contrast agents in the major organs, a biodistribution study was performed at 2 or 7 days postinjection of the agents in the mice bearing orthotopic 4T1 breast tumor. The tissues were dissolved in high purity nitric acid and the Gd(III) content was measured by ICP-OES. Fig. 10 shows the biodistribution of CREKA-Tris(Gd-DOTA)$_3$ or CERAK-Tris(Gd-DOTA)$_3$ in the major organs and tissues, including skin, muscle, femur, tumor, spleen, kidney, liver, lung, heart and brain, at 2 and 7 days after injection at a dose of 0.1 mmol-Gd/kg. The retention of both agents was comparable ($p > 0.05$) in the normal tissues and was statistically different ($p < 0.05$) in the tumor at 2 or 7 days post injection. The targeted agent displayed higher tumor uptake than the non-targeted agent. Most of the injected agents were eliminated from the body within the first 2 days post-injection. The kidneys and liver, the major organ involved in the excretion of agents,

had a Gd(III) retention of 1.50%, 0.82% of the injected CREKA-Tris(Gd-DOTA)$_3$ per gram of tissue, respectively, higher than other organs and tissues. The Gd(III) retention was further decreased to 0.38%, 0.48% of injected Gd(III) per gram of tissue in the kidneys and liver, respectively. No detectable Gd(III) was observed in the bone, muscle or brain for either agent. Compared to previously reported dendrimer-based targeted Gd(III) chelates, [22] the peptide targeted low molecular weight contrast agent has much lower Gd(III) retention. Dynamic three-dimensional maximum intensity projection MR images post injection of the contrast agents (Fig. 11) revealed rapid clearance of the peptide conjugates from the blood circulation and corresponding signal increase in the urinary bladder, indicating clearance of the agents via renal filtration. The rapid clearance of the peptide conjugates via renal filtration resulted in low tissue retention of the targeted contrast agent.

4. Conclusion

In summary, we developed a small molecular targeted contrast agent CREKA-Tris(Gd-DOTA)$_3$ for effective molecular MRI of a cancer biomarker abundant in the tumor microenvironment. CREKA specifically bound to the fibrin-fibronectin complexes in the tumor extracellular matrix. CREKA-Tris(Gd-DOTA)$_3$ resulted in strong and prolonged tumor contrast enhancement. The agent could be readily excreted via renal filtration and exhibited minimal long-term tissue retention. The small molecular peptide targeted MRI contrast agent has a great promise for clinical MR cancer molecular imaging.

Acknowledgments

The authors thank Dr. Chris Flask for technical assistance on MRI sequences. This work was supported in part by the NIH grant R01 CA097465.

References

1. Zhou Z, Lu ZR. Gadolinium-based contrast agents for magnetic resonance cancer imaging. Wires Nanomed Nanobi. 2013; 5:1–18.
2. Caravan P, Ellison JJ, McMurry TJ, Lauffer RB. Gadolinium(III) chelates as MRI contrast agents: structure, dynamics, and applications. Chem Rev. 1999; 99:2293–352. [PubMed: 11749483]
3. Chan KWY, Wong WT. Small molecular gadolinium(III) complexes as MRI contrast agents for diagnostic imaging. Coord Chem Rev. 2007; 251:2428–51.
4. Corot C, Robert P, Lancelot E, Prigent P, Ballet S, Guilbert I, et al. Tumor imaging using P866, a high-relaxivity gadolinium chelate designed for folate receptor targeting. Magn Reson Med. 2008; 60:1337–46. [PubMed: 19025883]
5. Marom H, Miller K, Bechor-Bar Y, Tsarfaty G, Satchi-Fainaro R, Gozin M. Toward development of targeted nonsteroidal antiandrogen-1,4,7,10-tetraazacyclododecane-1,4,7,10-tetraacetic acid-gadolinium complex for prostate cancer diagnostics. J Med Chem. 2010; 53:6316–25. [PubMed: 20715870]
6. Liu Y, Chen Z, Liu C, Yu D, Lu Z, Zhang N. Gadolinium-loaded polymeric nanoparticles modified with Anti-VEGF as multifunctional MRI contrast agents for the diagnosis of liver cancer. Biomaterials. 2011; 32:5167–76. [PubMed: 21521627]
7. Sipkins DA, Cheresh DA, Kazemi MR, Nevin LM, Bednarski MD, Li KCP. Detection of tumor angiogenesis in vivo by $\alpha_v\beta_3$-targeted magnetic resonance imaging. Nat Med. 1998; 4:623–6. [PubMed: 9585240]
8. Geninatti Crich S, Alberti D, Szabo I, Aime S, Djanashvili K. MRI visualization of melanoma cells by targeting overexpressed sialic acid with a Gd^{III}-dota-en-pba imaging reporter. Angew Chem Int Ed. 2012; 52:1161–4.

9. Accardo A, Tesauro D, Roscigno P, Gianolio E, Paduano L, D'Errico G, et al. Physicochemical properties of mixed micellar aggregates containing CCK peptides and Gd complexes designed as tumor specific contrast agents in MRI. J Am Chem Soc. 2004; 126:3097–107. [PubMed: 15012139]
10. Artemov D, Mori N, Ravi R, Bhujwalla ZM. Magnetic resonance molecular imaging of the HER-2/*neu* receptor. Cancer Res. 2003; 63:2723–7. [PubMed: 12782573]
11. Liu Y, Zhang N. Gadolinium loaded nanoparticles in theranostic magnetic resonance imaging. Biomaterials. 2012; 33:5363–75. [PubMed: 22521487]
12. Swanson SD, Kukowska-Latallo JF, Patri AK, Chen CY, Ge S, Cao ZY, et al. Targeted gadolinium-loaded dendrimer nanoparticles for tumor-specific magnetic resonance contrast enhancement. Int J Nanomed. 2008; 3:201–10.
13. Han L, Li J, Huang S, Huang R, Liu S, Hu X, et al. Peptide-conjugated polyamidoamine dendrimer as a nanoscale tumor-targeted T1 magnetic resonance imaging contrast agent. Biomaterials. 2011; 32:2989–98. [PubMed: 21277017]
14. Boyd AS, Zic JA, Abraham JL. Gadolinium deposition in nephrogenic fibrosing dermopathy. J Am Acad Dermatol. 2007; 56:27–30. [PubMed: 17109993]
15. Villaraza AJL, Bumb A, Brechbiel MW. Macromolecules, dendrimers, and nanomaterials in magnetic resonance imaging: the interplay between size, function, and pharmacokinetics. Chem Rev. 2010; 110:2921–59. [PubMed: 20067234]
16. Wang SJ, Brechbiel M, Wiener EC. Characteristics of a new MRI contrast agent prepared from polypropyleneimine dendrimers, generation 2. Invest Radiol. 2003; 38:662–8. [PubMed: 14501494]
17. Lu ZR, Wu X. Polydisulfide-based biodegradable macromolecular magnetic resonance imaging contrast agents. Isr J Chem. 2010; 50:220–32. [PubMed: 21331318]
18. Neri D, Carnemolla B, Nissim A, Leprini A, Querze G, Balza E, et al. Targeting by affinity-matured recombinant antibody fragments of an angiogenesis associated fibronectin isoform. Nat Biotechnol. 1997; 15:1271–5. [PubMed: 9359110]
19. Croix BS, Rago C, Velculescu V, Traverso G, Romans KE, Montgomery E, et al. Genes expressed in human tumor endothelium. Science. 2000; 289:1197–202. [PubMed: 10947988]
20. Wu X, Burden-Gulley SM, Yu G, Tan M, Lindner D, Brady-Kalnay SM, et al. Synthesis and evaluation of a peptide targeted small molecular Gd-DOTA monoamide conjugate for MR molecular imaging of prostate cancer. Bioconjugate Chem. 2012; 23:1548–56.
21. Tan M, Burden-Gulley SM, Li W, Wu X, Lindner D, Brady-Kalnay SM, et al. MR molecular imaging of prostate cancer with a peptide-targeted contrast agent in a mouse orthotopic prostate cancer model. Pharm Res. 2011; 20:953–60. [PubMed: 22139536]
22. Tan M, Wu X, Jeong EK, Chen Q, Lu ZR. Peptide-targeted nanoglobular Gd-DOTA monoamide conjugates for magnetic resonance cancer molecular imaging. Biomacromolecules. 2010; 11:754–61. [PubMed: 20131758]
23. Cheng Z, Al Zaki A, Hui JZ, Muzykantov VR, Tsourkas A. Multifunctional nanoparticles: cost versus benefit of adding targeting and imaging capabilities. Science. 2012; 338:903–10. [PubMed: 23161990]
24. Wedeking P, Tweedle M. Comparison of the biodistribution of ^{153}Gd-labeled $Gd(DTPA)^{2-}$, $Gd(DOTA)^{-}$, and $Gd(Acetate)_n$ in mice. Nucl Med Biol. 1988; 15:395–402.
25. White GW, Gibby WA, Tweedle MF. Comparison of Gd(DTPA-BMA) (Omniscan) versus Gd(HP-DO3A) (ProHance) relative-to gadolinium retention in human bone tissue by inductively coupled plasma mass spectroscopy. Invest Radiol. 2006; 41:272–8. [PubMed: 16481910]
26. Ye Z, Wu X, Tan M, Jesberger J, Griswold M, Lu Z-R. Synthesis and evaluation of a polydisulfide with Gd–DOTA monoamide side chains as a biodegradable macromolecular contrast agent for MR blood pool imaging. Contrast Media Mol I. 2013; 8:220–8.
27. Pilch J, Brown DM, Komatsu M, Jarvinen TA, Yang M, Peters D, et al. Peptides selected for binding to clotted plasma accumulate in tumor stroma and wounds. Proc Natl Acad Sci USA. 2006; 103:2800–4. [PubMed: 16476999]
28. Simberg D, Duza T, Park JH, Essler M, Pilch J, Zhang L, et al. Biomimetic amplification of nanoparticle homing to tumors. Proc Natl Acad Sci USA. 2007; 104:932–6. [PubMed: 17215365]

29. Mastarone DJ, Harrison VSR, Eckermann AL, Parigi G, Luchinat C, Meade TJ. A modular system for the synthesis of multiplexed magnetic resonance probes. J Am Chem Soc. 2011; 133:5329–37. [PubMed: 21413801]

30. Chabre YM, Contino-Pepin C, Placide V, Shiao TC, Roy R. Expeditive synthesis of glycodendrimer scaffolds based on versatile TRIS and mannoside derivatives. J Org Chem. 2008; 73:5602–5. [PubMed: 18572921]

31. Mantovani G, Lecolley F, Tao L, Haddleton DM, Clerx J, Cornelissen JJLM, et al. Design and synthesis of N-maleimido-functionalized hydrophilic polymers via copper-mediated living radical polymerization: A suitable alternative to PEGylation chemistry. J Am Chem Soc. 2005; 127:2966–73. [PubMed: 15740133]

32. Boros E, Caravan P. Structure-relaxivity relationships of serum albumin targeted MRI probes based on a single amino acid Gd complex. J Med Chem. 2013; 56:1782–6. [PubMed: 23391162]

33. Caravan P. Protein-targeted gadolinium-based magnetic resonance imaging (MRI) contrast agents: design and mechanism of action. Acc Chem Res. 2009; 42:851–62. [PubMed: 19222207]

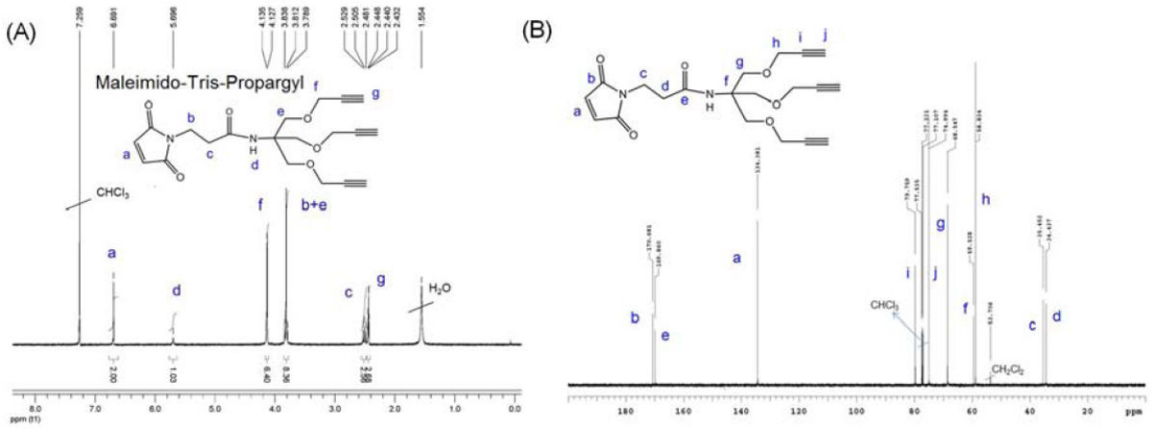

Fig. 1.

^{1}H NMR (A) and ^{13}C NMR (B) spectra of Maleimido-Tris-Propargyl in $CDCl_3$.

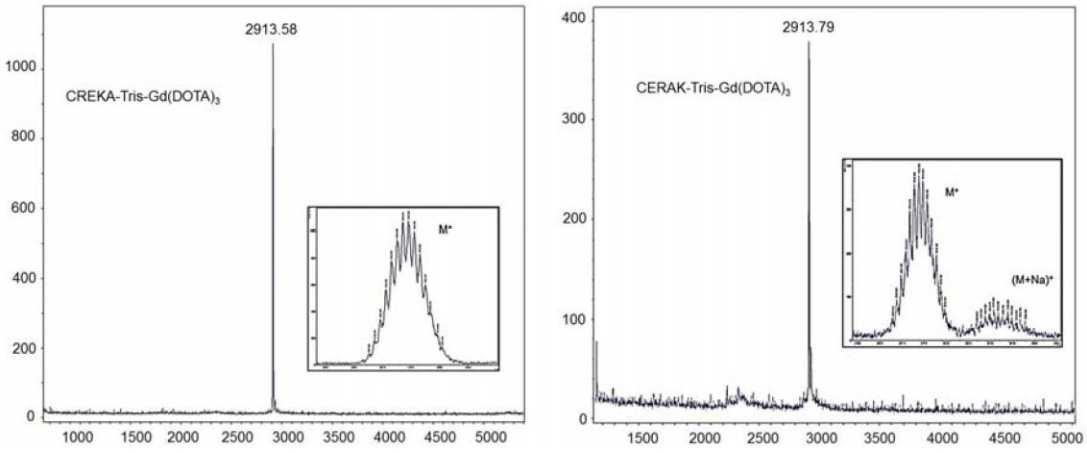

Fig. 2.

The MALDI-TOF MS spectra of the CREKA-Tris(Gd-DOTA)$_3$ and CERAK-Tris(Gd-DOTA)$_3$.

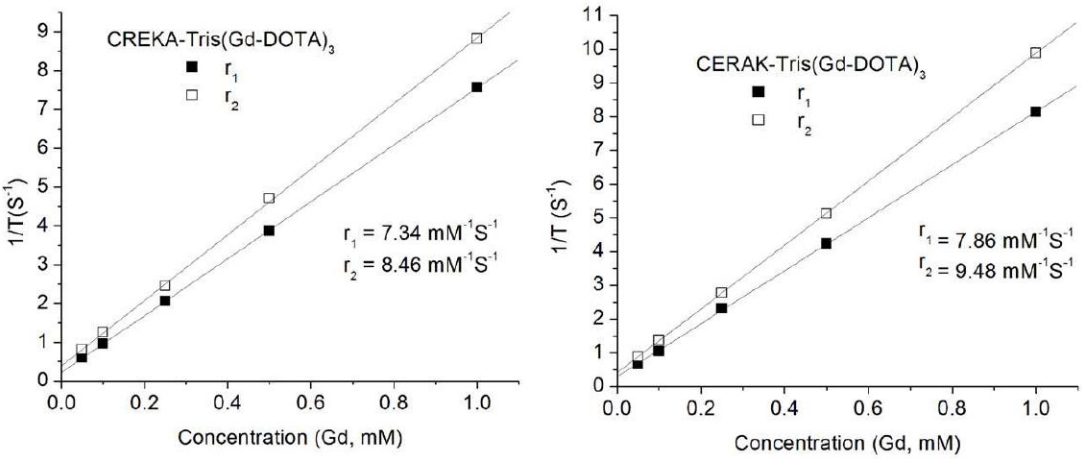

Fig. 3.

The plots of $1/T_1$ and $1/T_2$ versus the concentration of CREKA-Tris(Gd-DOTA)$_3$ and CERAK-Tris(Gd-DOTA)$_3$.

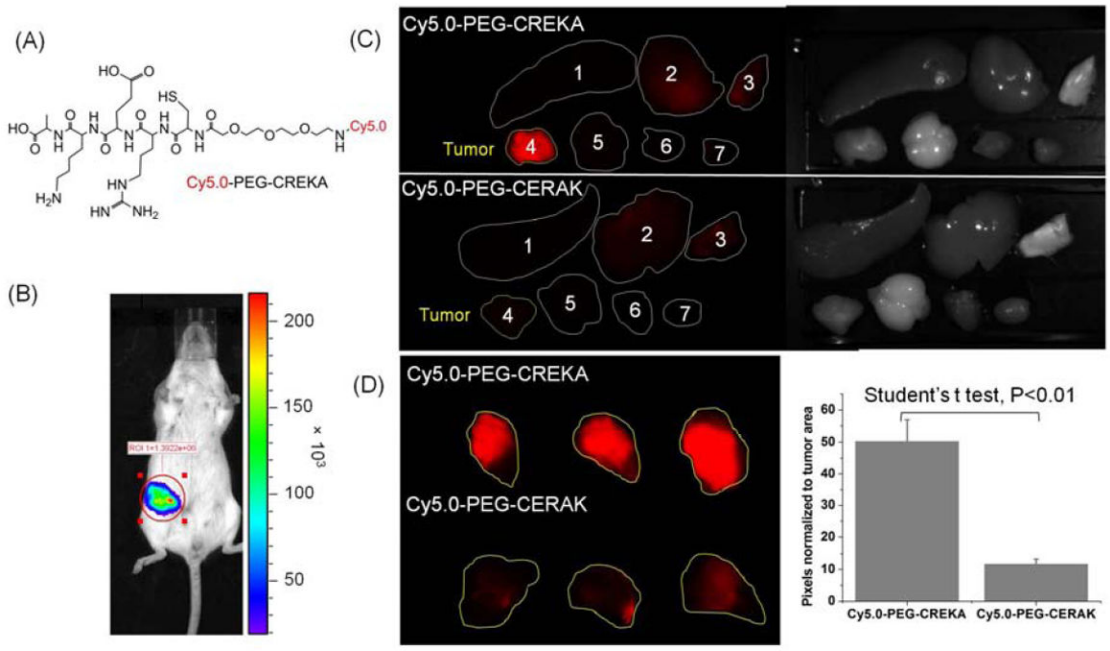

Fig. 4.

(A) The structure of Cy5.0-PEG-CREKA. (B) Bioluminescence images showing mice bearing 4T1-Luc breast tumor in mammary fat pad two weeks after implantation. Mice were intraperitoneally injected with D-luciferin (150 mg/kg body weight) 10 min before imaging with Xenogen IVIS Lumina system. (C) Mice bearing 4T1-GFP-Luc2 breast tumor were intravenously injected with Cy5.0-PEG-CREKA or Cy5.0-PEG-CERAK (0.3 μmol/kg body weight). After 4 h, the mice were sacrificed and the tumors and various organs (1. Spleen, 2. Liver, 3. Lung, 4. Tumor, 5. Brain, 6. Muscle, 7. Heart) were imaged with the Maestro FLEX In Vivo Imaging System. (D) Tumors of mice injected with Cy5.0-PEG-CREKA or Cy5.0-PEG-CERAK were imaged side by side with the Maestro FLEX *In Vivo* Imaging System and the pixels normalized to tumor area were analyzed with Maestro software (n = 3).

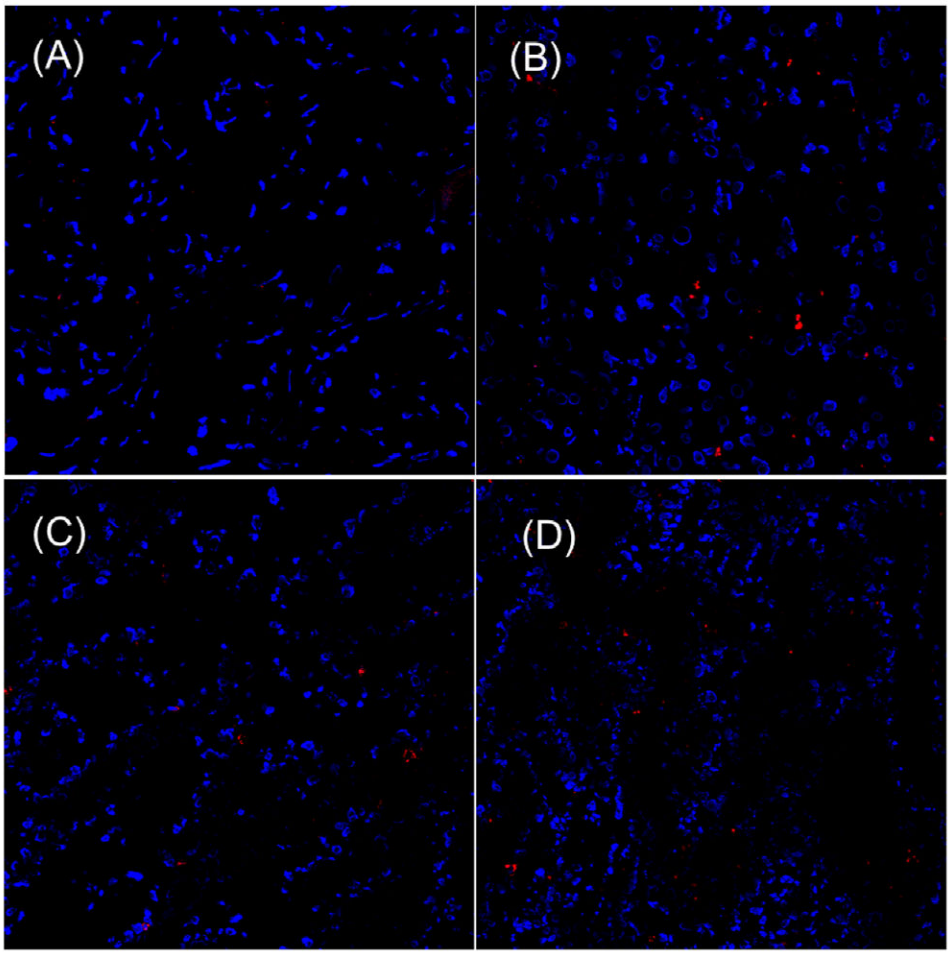

Fig. 5.

Histological analysis of heart (A), liver (B), lung (C) and spleen (D), from mouse 5 h after injection of 300 nmol/kg of CREKA-PEG-Cy5.0. (cell nuclei was stained by DAPI, blue; Cy5.0 was shown as red).

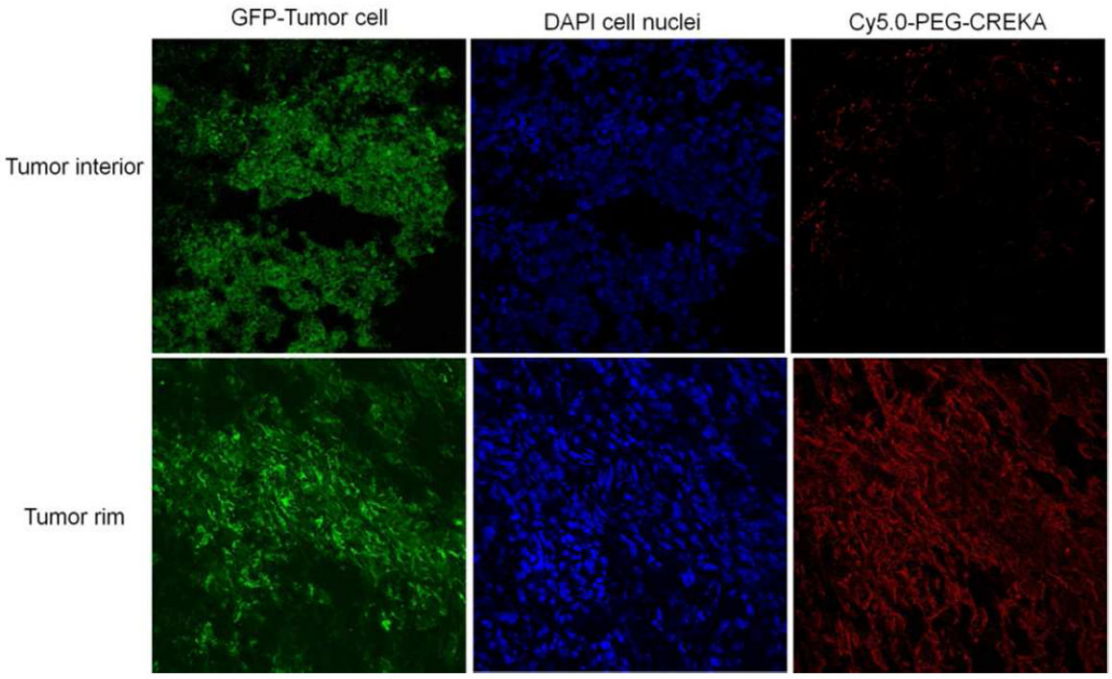

Fig. 6.

Frozen section of 4T1-GFP-Luc2 breast tumor interior or rim from mouse injected with Cy5.0-PEG-CREKA. The slides were imaged by confocal microscopy.

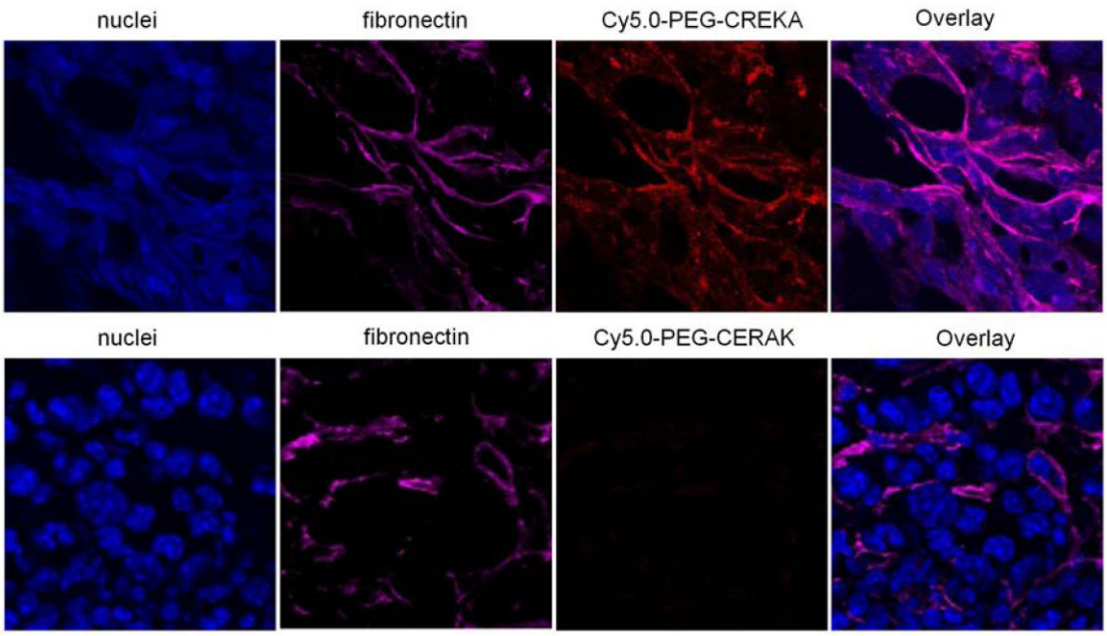

Fig. 7.

Frozen section of 4T1-GFP-Luc2 breast tumor from mice injected with Cy5.0-PEG-CREKA or Cy5.0-PEG-CERAK were stained for fibronectin.

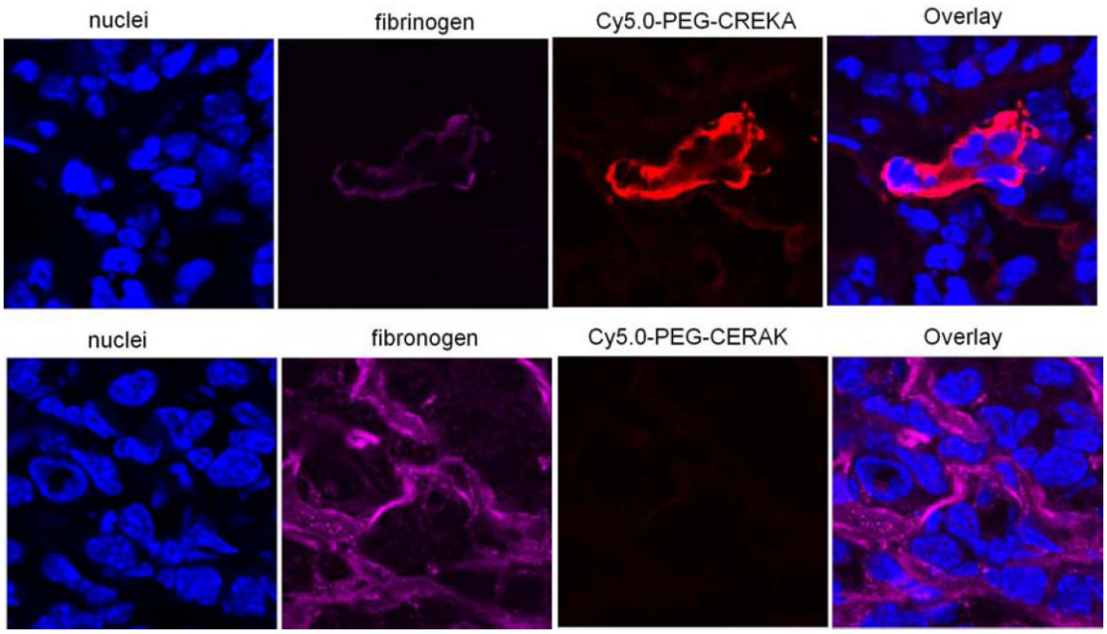

Fig. 8.

Frozen section of 4T1-GFP-Luc2 breast tumor from mice injected with Cy5.0-PEG-CREKA or Cy5.0-PEG-CERAK were stained for fibrinogen.

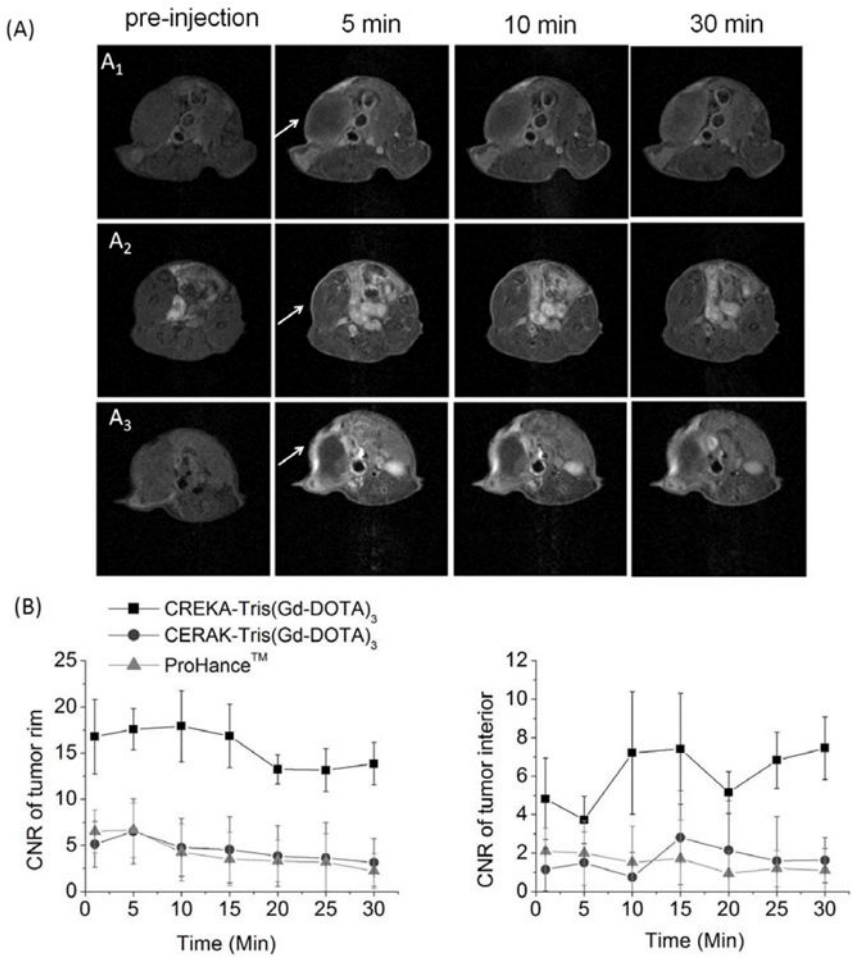

Fig. 9.

(A) Representative 2D axial T_1-weighted MR images of mice bearing 4T1-GFP-Luc2 breast tumor before (pre) and at 1, 10, 30 minutes after injection of Prohance™ (A_1), CERAK-Tris(Gd-DOTA)$_3$ (A_2), or CREKA-Tris(Gd-DOTA)$_3$ (A_3), at 0.1 mmol-Gd/kg. White arrows point to the primary tumor. (B) Contrast-to-noise ratio (CNR) in the tumor rim or interior with Prohance™, CREKA-Tris(Gd-DOTA)$_3$ or CERAK-Tris(Gd-DOTA)$_3$ administered at 0.1 mmol-Gd/kg in the orthotopic 4T1-GFP-Luc2 breast tumor bearing mice (N=3).

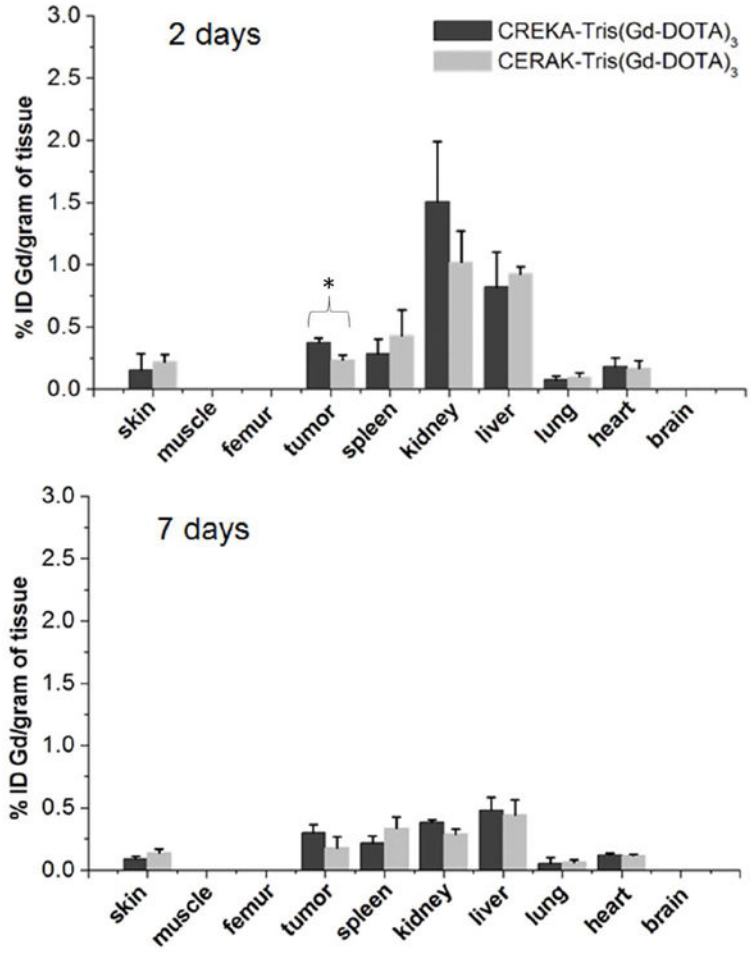

Fig. 10.

Biodistribution of gadolinium in the major organs and tissues of mice at 2 or 7 days after intravenous injection of CREKA-Tris(Gd-DOTA)$_3$ or CERAK-Tris(Gd-DOTA)$_3$ at a dose of 0.1 mmol-Gd/kg in mice (n = 3) bearing orthotopic 4T1-GFP-Luc2 breast tumor (* $p < 0.05$).

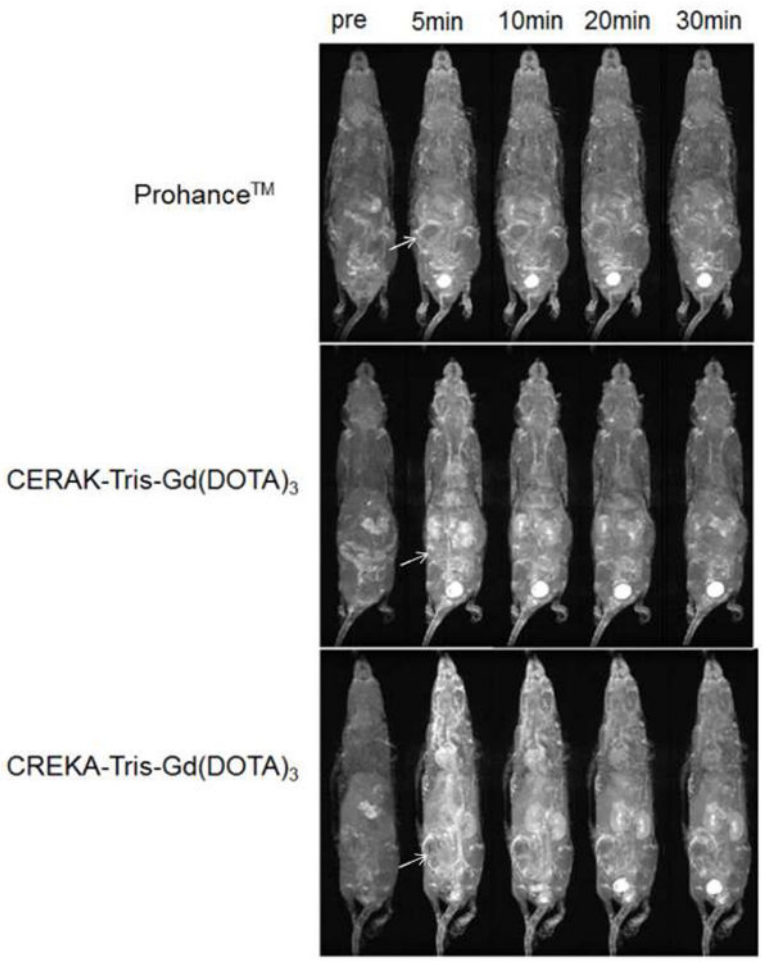

Fig. 11.

Representative 3D maximum intensity projection images (T_1-weighted) of a4T1-GFP-Luc2 breast tumor bearing mice injected with Prohance™, CREKA-Tris(Gd-DOTA)$_3$ or CERAK-Tris(Gd-DOTA)$_3$ at 0.1 mM-Gd/kg. White arrows show tumor.

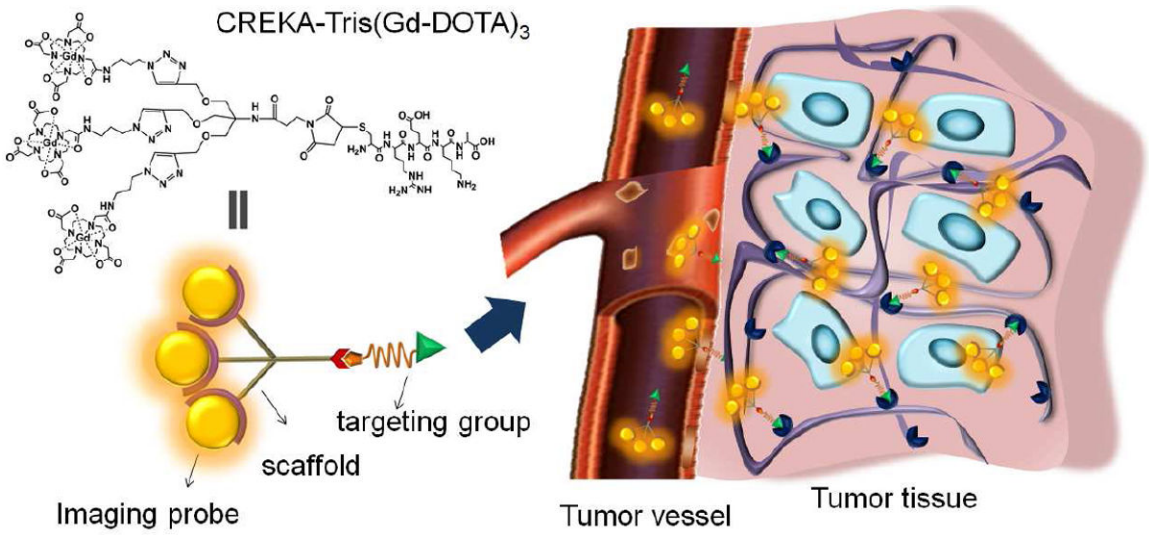

Scheme 1.

The structure of CREKA-Tris(Gd-DOTA)$_3$ and the illustration of its binding to the fibrin-fibronectin complex in tumor extracellular matrix for MR signal enhancement.

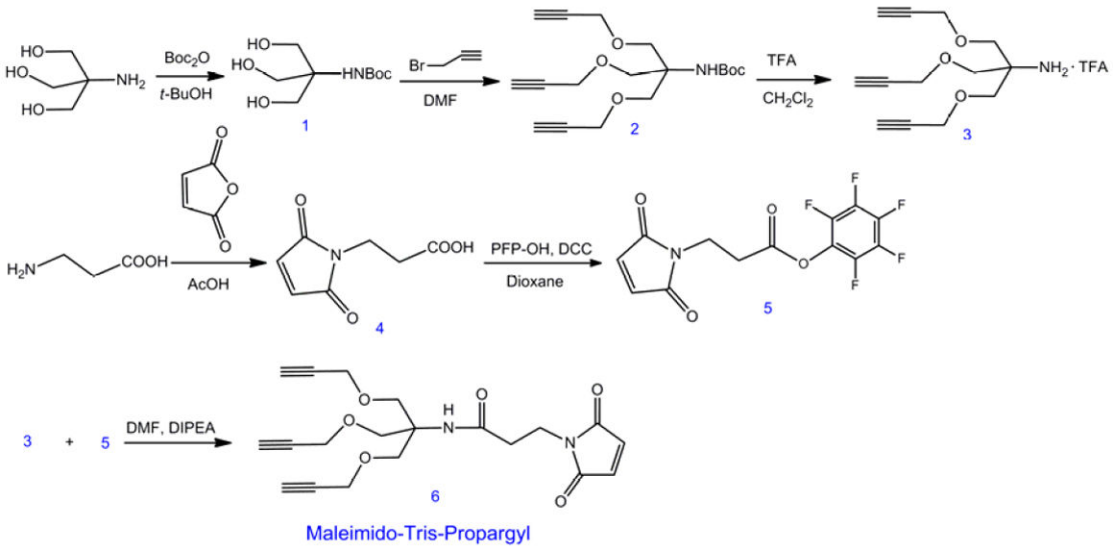

Scheme 2.
The synthesis of Maleimido-Tris-Propargyl.

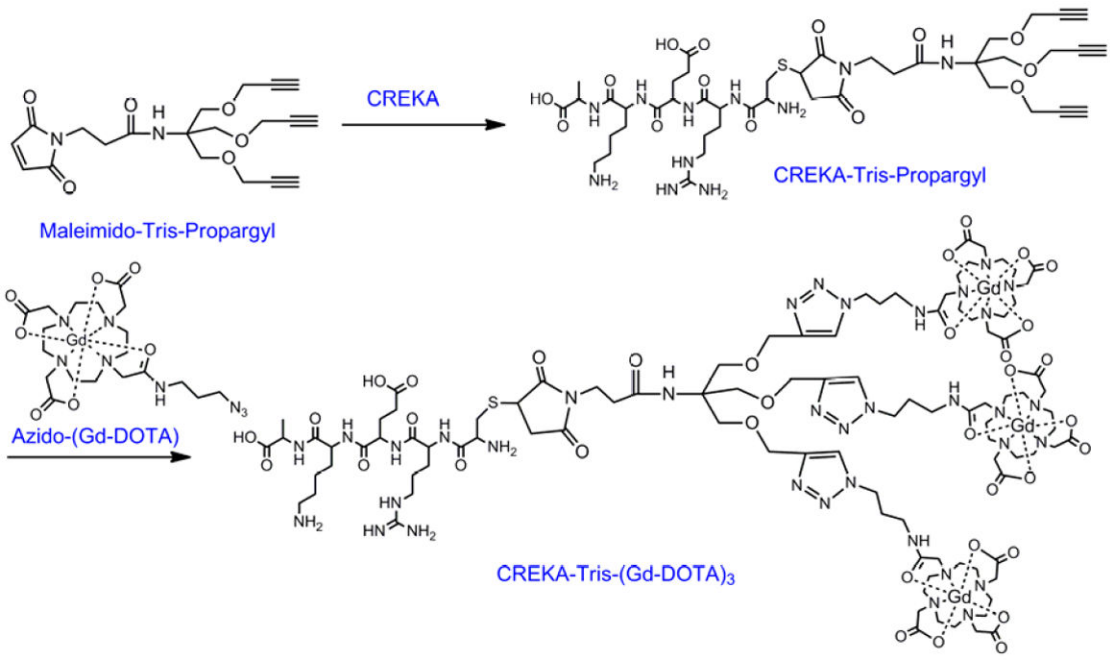

Scheme 3.

The synthesis of Synthesis of CREKA-Tris(Gd-DOTA)$_3$ and CERAK-Tris(Gd-DOTA)$_3$.